

## AL46 - Simulation and Analysis of the Impact of Current Variations on Electrothermal Balance in Aluminum Electrolysis Cell

Ao Hongmin<sup>1</sup>, He Song<sup>2</sup>, Yan Feiya<sup>3</sup> and Liu Zheng<sup>4</sup>

1. Design engineer

2. Group leader

3. Department head

4. Department head

Guiyang Aluminum Magnesium Design and Research Institute Co., Ltd., Guiyang, China.

Corresponding author: ahm1989@126.com

### Abstract

With the worsening of energy shortage, aluminum electrolysis plants in some areas will face the problem of power shortage, which will lead to variations in the current of electrolytic cells. At the same time, some aluminum smelters are increasing their metal production by strengthening cell design. This will affect the electrical distribution of the aluminum electrolytic cell, but the electrical balance of the aluminum cell is crucial to the electrolytic production. In this paper, the changes of voltage distribution, energy consumption and temperature distribution of 500 kA aluminum electrolysis cells are analyzed in detail when the current fluctuates within  $\pm 10\%$  by using ANSYS software.

**Keywords:** Aluminum electrolytic cell, Electrothermal balance, ANSYS simulation calculation, Current variations.

### 1. Introduction

Aluminum production is an energy-intensive process, and aluminum electrolytic cells are an important part of the production line. Maintaining the electrothermal balance of the aluminum electrolytic cell is essential to ensure efficiency of aluminum production and minimize energy consumption. Due to power constraints and cell upgrades, electrolytic plants may face the problem of variations in the cell current. Understanding the effect of current variations on thermal balance is critical to optimizing the operation and production efficiency of aluminum electrolysis processes.

In this paper, the influence of current variations on thermal balance in 500 kA aluminum electrolytic cell is analyzed by using ANSYS simulation software.

### 2. Mathematical Model and Simulation Condition of Cell Electrothermal Field

#### 2.1 Electric Model

The cell voltage of aluminum electrolysis cell is mainly composed of the following parts, as shown in Equation (1):

$$V_{\text{Cell}} = V_{\text{ACD}} + V_{\text{Anode}} + V_{\text{Cathode}} + V_{\text{Busbar}} + BEMF \quad (1)$$

where:

$V_{\text{Cell}}$  Average cell voltage, including voltage adders and anode effects, V

$V_{\text{ACD}}$  Voltage drop between anode and cathode, comprising bath and bubble voltage drops, V

|                      |  |
|----------------------|--|
| $V_{\text{Anode}}$   | Anode voltage drop, V  |
| $V_{\text{Cathode}}$ | Cathode voltage drop, V  |
| $V_{\text{Busbar}}$  | Busbar voltage drop from end of collector bars in one cell to anode rods below the anode beam on the downstream adjacent cell, V |

The potline busbar linkage voltage drop, comprising passageways and crossovers is not included in Equation (1) because it does not belong to any cell, and does not participate in cell heat balance. However, it has to be included in the overall energy consumption of the cell.

## 2.2 Energy Balance Model

The cell generates a large amount of energy from the current, which is necessary to maintain the electrochemical reaction. In addition, energy balance also includes the overall heat loss from the cell and the heat required for electrochemical reactions. The heat loss of the cell is generally divided into three parts: heat loss from the top of the cell, heat loss from the side of the cell and heat loss from the bottom of the cell [1].

## 2.3 Governing Equation

### (1) Differential Equation of Electric Potential

Under normal production conditions, the current does not fluctuate. The transmission speed of the current is very fast without lag. As a result, the conductive process can be represented with a 3D Laplace Equation (2) [2]:

$$\frac{\partial}{\partial x} \left[ \frac{1}{\rho_x} \frac{\partial V}{\partial x} \right] + \frac{\partial}{\partial y} \left[ \frac{1}{\rho_y} \frac{\partial V}{\partial y} \right] + \frac{\partial}{\partial z} \left[ \frac{1}{\rho_z} \frac{\partial V}{\partial z} \right] = 0 \quad (2)$$

where:

|                          |  |
|--------------------------|--|
| $\rho_x, \rho_y, \rho_z$ | Resistivities of the material in x, y and z, respectively, $\Omega \cdot \text{mm}^2/\text{m}$ |
| V                        | Electrical potential, V  |

### (2) Differential Equation of Heat Conduction

Heat transfer in the cell follows the Poisson heat conduction equation with electric internal heat source, Equation (3) [3, 4]:

$$\frac{\partial}{\partial x} \left[ k_x \frac{\partial T}{\partial x} \right] + \frac{\partial}{\partial y} \left[ k_y \frac{\partial T}{\partial y} \right] + \frac{\partial}{\partial z} \left[ k_z \frac{\partial T}{\partial z} \right] + q = 0 \quad (3)$$

where:

|                 |  |
|-----------------|--|
| $k_x, k_y, k_z$ | Thermal conductivities in the 3 directions, respectively, which vary with temperature, W/(m·K) |
| q               | Volumetric heat generation rate of internal heat source per second, W/m <sup>3</sup>           |
| T               | Temperature, K.  |

q in Equation (3) refers to the joule heat generated by the current passing through per second, so it is relevant to the potential in Equation (2) and the two equations need to be coupled for solution.

The calculation of the cell electrothermal field involves solution of both equations (2) and (3). In this paper, the cell model is established for the electrothermal field of 500 kA cell by using the finite element software ANSYS.

## 2.4 Calculation Boundary Condition

In this paper, the electrothermal distribution of the cell under normal operation of 500 kA current is calculated first. On this basis, the influence of current variations on the electrothermal distribution are studied by changing the current. Figure 1 shows the 500 kA cell model. In the actual production process, after the current of the cell changes, the relevant production process parameters may be adjusted to ensure the normal operation of the cell. However, this paper mainly studies the effect of current variations on the electrothermal balance of an electrolytic cell, so only the current is changed based on a 500 kA electrolytic cell, and the other boundary conditions and production process parameters remain unchanged.

The anode cover thickness was 17 cm for the base case of 500 kA, and as in practice, it was increased at 450 kA and decreased at 550 kA, in order to balance the heat and keep ledge protection on the walls of the cathode cavity.

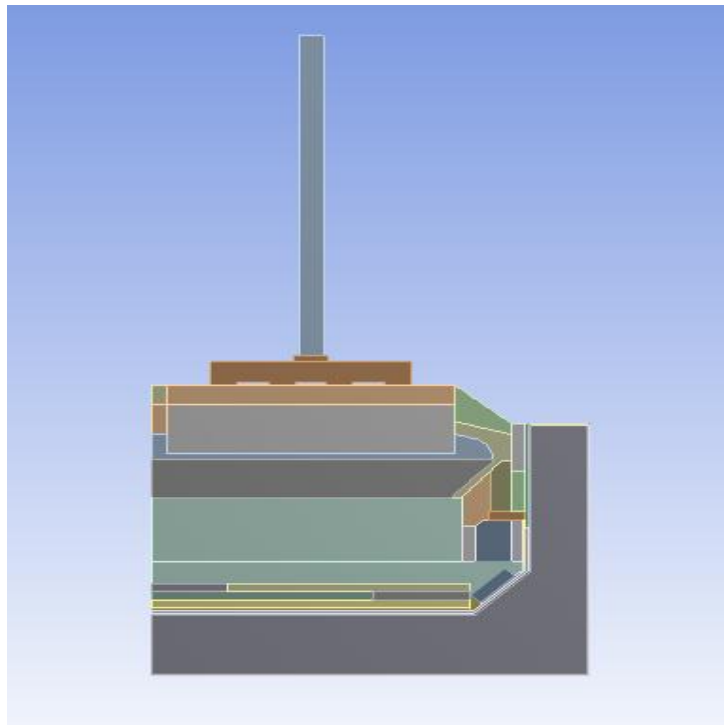


**Figure 1. 500 kA cell model.**

The base case of 500 kA, the current is increased and decreased by 25 kA in the range of 450 kA to 550 kA. The voltage distribution, energy consumption distribution and temperature distribution of the electrolytic cell under these different currents are calculated and analyzed.

## 3. Results, Analysis and Discussion

### 3.1 Voltage Breakdown and Heat Balance of 500 kA Cell

Through the calculation of electrothermal field, the voltage drop breakdown of 500 kA cell is given in Table 1.

**Table 1. 500 kA voltage balance.**

| Item  | Voltage drop value (V) |
|---|------------------------|
| Anode voltage drop  | 0.355                  |
| Cathode voltage drop                                      | 0.235                  |
| Cell busbar voltage drop                                  | 0.265                  |
| Voltage drop in the ACD space, including bath and bubbles | 1.266                  |
| Back EMF (BEMF)*  | 1.787                  |
| Cell voltage  | 3.908                  |

\*These voltages were calculated, using Haupin [5].

As shown in Table 1, cell voltage is 3.908 V, and the voltage drop is distributed in a reasonable manner in all parts.

The cell heat balance is based on the concept of internal heat, defined in Equation (4) [6, 7].

$$Q_{int} = [V_{Cell} - V_{Busbar} - (V_{Al} + V_{aux})]I \quad (4)$$

where:

$Q_{int}$  Cell internal heat, kW

$V_{Cell}$  Cell voltage, V

$V_{Busbar}$  Busbar voltage drop outside the System Boundary 2 in Figure 2, V

$V_{Al}$  Voltage equivalent of enthalpy to make aluminium, given in Equation (5), V

$V_{aux}$  Voltage equivalent of heat removed from the cell by auxiliary processes, such as anode butt removal, cavity scoop, aluminium fluoride and impurity additions, etc., including the heat generated by some percentage of net carbon consumption (air-burn of the anodes), V

$I$  Cell current, kA.

$V_{aux}$  has to be evaluated for each technology; in this work we assumed it to be 0.035 V.

Cell internal heat is the net heat within the control volume, which has to be lost through the control volume boundaries; for this paper, we use System Boundary 2 (Figure 2)

$V_{Al}$ , the voltage equivalent of enthalpy to make aluminium is given in Equation (5) [6],

$$V_{Al} = 0.450 + 3.110 \times 10^{-5} T + [1.4316 - 0.03252(1 - \varepsilon) + 2.255 \times 10^{-4} T] \eta \quad (5)$$

where:

$T$  Bath temperature, °C

$\eta$  Current efficiency, fraction

$\varepsilon$  Fraction of alpha alumina in alumina.

Table 2 gives the internal heat and voltages for the five cases studied.

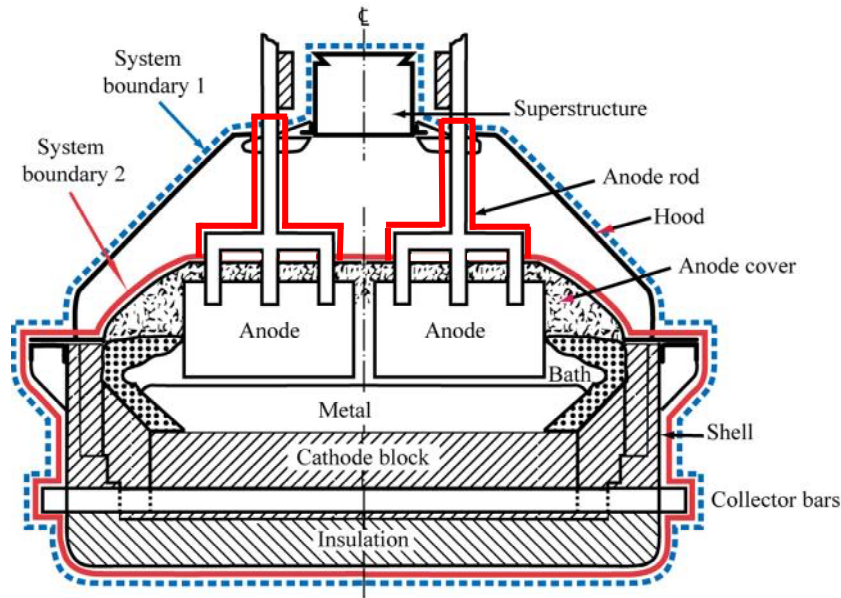


Figure 2. System boundaries of control volumes, delimiting internal heat and heat loss.

### 3.2 Voltage Distribution Analysis

From the base case of 500 kA, cell the voltage drop breakdown for different currents is given in Table 2. For simplicity, the anode, cathode and busbar voltage drops are assumed to be proportional to the current, which is by a few mV different than obtained with ANSYS model.

Table 2. Voltage distribution for different currents, assuming constant anode-cathode distance (ACD) from the base case = 3.70 cm.

| Current<br>kA | Anode<br>current<br>density<br>A/cm <sup>2</sup> | Anode<br>voltage<br>drop<br>(V) | Cathode<br>voltage<br>drop<br>(V) | Busbar<br>voltage<br>drop<br>(V) | Bath and<br>bubble<br>voltage drop<br>(V) | BEMF<br>(V)  | Cell<br>voltage<br>(V) |
|---------------|--|---------------------------------|-----------------------------------|----------------------------------|---|--------------|------------------------|
| 450           | 0.69   | 0.320                           | 0.212                             | 0.239                            | 1.140                                     | 1.773        | 3.682                  |
| 475           | 0.73   | 0.337                           | 0.223                             | 0.252                            | 1.203                                     | 1.780        | 3.784                  |
| <b>500</b>    | <b>0.76</b>                                      | <b>0.355</b>                    | <b>0.235</b>                      | <b>0.265</b>                     | <b>1.266</b>                              | <b>1.787</b> | <b>3.908</b>           |
| 525           | 0.80   | 0.373                           | 0.247                             | 0.278                            | 1.329                                     | 1.794        | 4.020                  |
| 550           | 0.84   | 0.391                           | 0.259                             | 0.292                            | 1.392                                     | 1.800        | 4.132                  |

It can be seen from Table 2 that for constant ACD, when the current is reduced from 500 kA to 450 kA, the cell voltage is reduced from 3.908 V to 3.682 V, and the voltage drop of each part of the cell also shows the same decreasing trend. When the current is increased from 500 kA to 550 kA, the working voltage of the cell is increased from 3.908 V to 4.132 V, and the voltage drop of each part of the cell also showed the same increasing trend.

The anode, electrolyte and cathode current density changes with the increase or decrease of current of electrolytic cell, so the voltage drop value of each part also changes correspondingly. This simulation calculation does not adjust the ACD, so the electrolyte voltage drop also increases with the increase of the current density. The variation trend of the voltage drop of each part of the

electrolysis cell is shown in Figure 3, and the variation trend of the operating voltage of the electrolysis cell is shown in Figure 4.

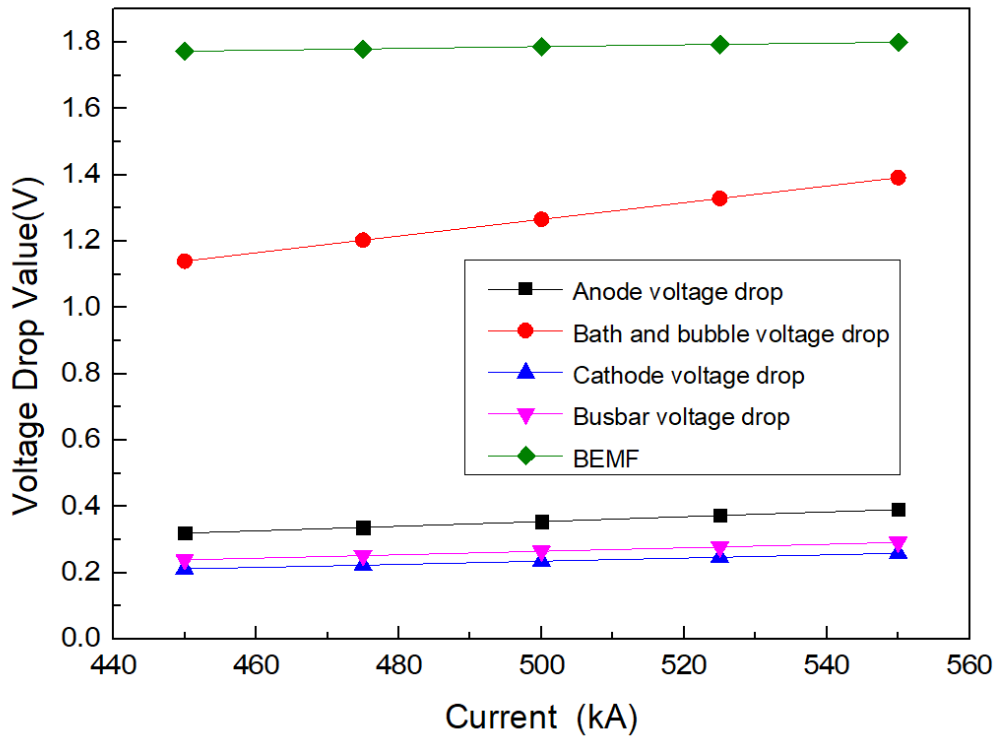


Figure 3. Voltage variation trend of each part of the electrolytic cell.

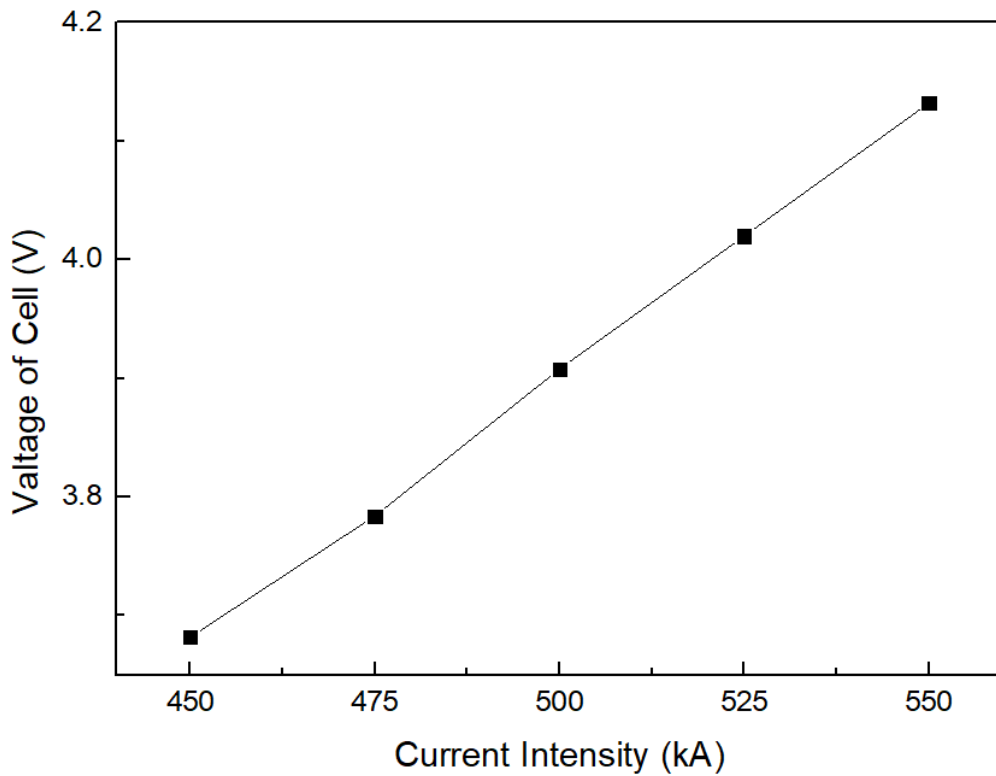


Figure 4. Variation trend of operating voltage of electrolytic cell, assuming constant ACD.

### 3.3 Impact of Energy Consumption Distribution

Figure 5 shows the temperature distribution contours of the 500 kA cell. In this paper, the heat distribution of three important areas of the potshell is analyzed, as shown in Figure 6. The maximum temperature of the potshell is 302 °C, the maximum temperature of the lower potshell is 118 °C, and the maximum temperature of the bottom potshell is 73 °C.

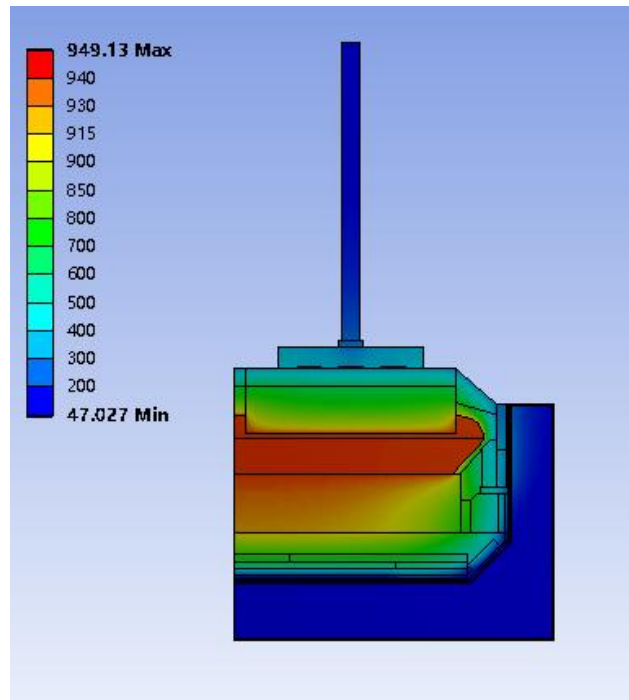


Figure 5. Temperature distribution of the 500 kA cell.

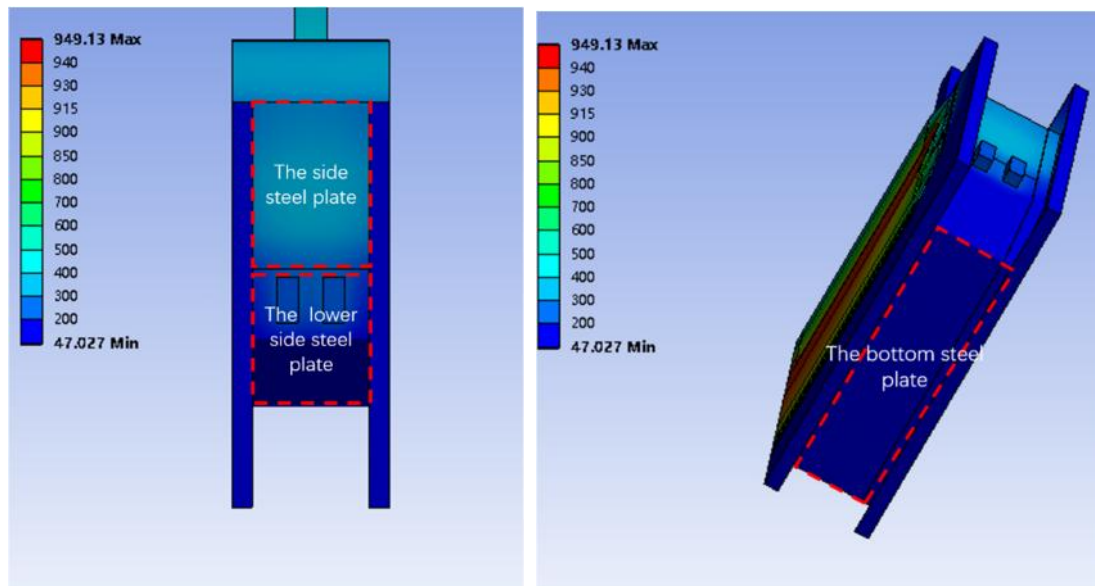


Figure 6. Three important areas of the cell shell.

The total heat dissipation of 500 kA cell is 829 kW, in which the heat loss through the anodes is 431.1 kW, and the heat dissipation through the cathode is 397.9 kW. Table 3 shows the heat balance for different currents.

**Table 3. Heat balance for different currents at constant ACD.  $V_{aux} = 0.035$  V in all cases.**

| Current (kA) | $V_{Al} + V_{aux}$ | $Q_{in}$   | Heat loss through the anodes |           | Heat loss through the cathode |           | Thickness of side ledge | Total heat loss in ANSYS |
|--------------|--------------------|------------|------------------------------|-----------|-------------------------------|-----------|-------------------------|--------------------------|
|              |                    |            | kW                           | %         | kW                            | %         |                         |                          |
| Item         | V                  | kW         | kW                           | %         | kW                            | %         | cm                      | kW                       |
| 450          | 1.985              | 656        | 393.6                        | 60        | 262.4                         | 40        | 18.5                    | 656                      |
| 475          | 1.985              | 740        | 414.4                        | 56        | 325.6                         | 44        | 15.1                    | 740                      |
| <b>500</b>   | <b>1.985</b>       | <b>829</b> | <b>431.1</b>                 | <b>52</b> | <b>397.9</b>                  | <b>48</b> | <b>12.5</b>             | <b>829</b>               |
| 525          | 1.985              | 922        | 461.0                        | 50        | 461.0                         | 50        | 9.3                     | 922                      |
| 550          | 1.985              | 1020       | 479.4                        | 47        | 540.6                         | 53        | 4.3                     | 1020                     |

The  $V_{Al} + V_{aux}$  remains constant according to Equation (5), because the bath temperature, current efficiency and percent alpha-alumina are kept constant.

As can be seen from Table 3, when the current is reduced to 450 kA, internal heat is 656 kW, the heat lost through the anodes is 393.60 kW, and the heat lost through the cathode is 262.4 kW. Compared with the 500 kA cell, the overall internal heat of the cell is reduced by 173 kW, the heat loss and percentage of each part is reduced. The heat lost through the anodes is mainly related to the thickness of the covering material on the anodes, and the temperature distribution in the anode region.

In this calculation process, the covering material on the cell does not change. Heat dissipation in the anode region is reduced mainly because the temperature distribution in the anode region is reduced after the current is reduced, but the reduction is small. The variation of heat lost through the cathode is mainly related to the ledge formed on the lining sidewalls. The energy consumption variation trend of each part caused by current change is shown in Figure 7.

As can be seen from Figure 7, the heat lost through the cathode is basically the same as that in the anode region. The trend of current change is positively correlated with total energy consumption and energy consumption of each part.

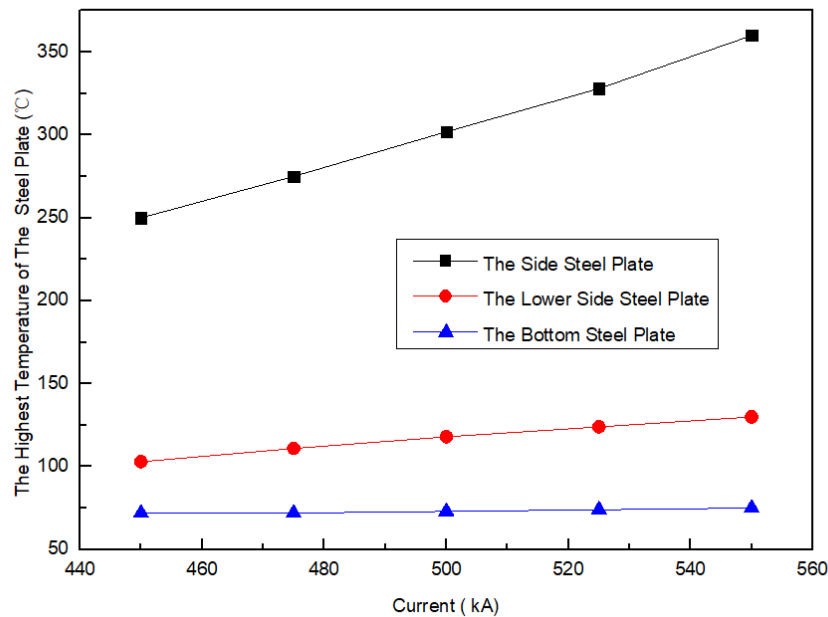


**Figure 7. Trend chart of energy consumption of each part caused by current change.**

### 3.4 Analysis of Influence of Temperature Distribution

By calculating the temperature distribution of the 500 kA cell, the maximum temperature of the potshell is 302 °C, the maximum temperature of the lower potshell is 118 °C, and the maximum temperature of the bottom potshell is 73 °C. Under different currents, the temperature changes are shown in Table 4.

**Table 4. Temperature distribution for different currents.**

| Current (kA) | Maximum temperature of the side potshell (°C) | Maximum temperature of the lower side potshell (°C) | Maximum temperature of bottom potshell (°C) |
|--------------|---|---|---|
| 450          | 250   | 103   | 72  |
| 475          | 275   | 111   | 72  |
| <b>500</b>   | <b>302</b>                                    | <b>118</b>  | <b>73</b>                                   |
| 520          | 328   | 124   | 74  |
| 550          | 360   | 130   | 75  |

As can be seen from Table 4, the change of current has a significant impact on the maximum temperature of the side potshell. When the current is reduced to 450 kA, the maximum temperature of the lower side potshell is 250 °C, which is reduced by 55 °C. When the current is increased to 550 kA, the highest temperature of the side potshell is 360 °C, an increase of 58 °C. The main reason is that the thickness of the frozen ledge changes: when the current increases, the electrolyte current density increases, the frozen ledge becomes thinner and the side temperature increases. When the current decreases, the electrolyte current density decreases, the frozen ledge thickens, and the side temperature decreases. At the same time, it can be seen from Table 4 that the change of current has little influence on the maximum temperature of the bottom potshell of the measurement, mainly because the thermal resistance of the lining in the bottom potshell region is large, resulting in a small change in the external temperature. The variation trend of temperature distribution in each part is shown in Figure 8.

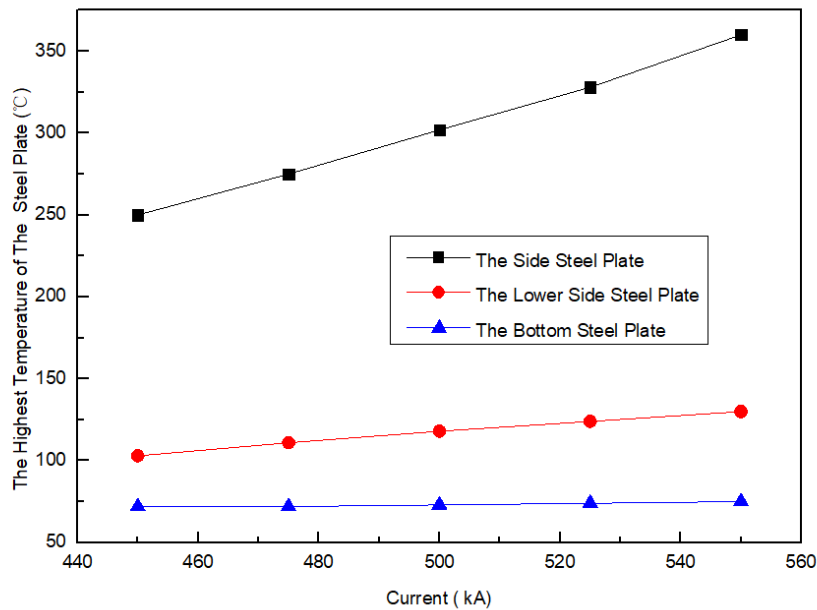


**Figure 8. Trend chart of temperature distribution of each part.**

#### 4. Conclusions

The influence of current variations on electrothermal balance of 500 kA cell was analyzed by ANSYS simulation. The results show that when the current decreases, the voltage of the cell decreases, the energy consumption distribution decreases, the maximum temperature of the side potshell decreases, and the temperature of the bottom and the lower side potshell changes little. When the current increases, the voltage of the electrolytic cell increases, the energy consumption increases correspondingly, the maximum temperature of the side potshell increases, and the temperature of the bottom and lower side potshell changes little. This calculation is based on a single factor change calculation, by varying cell current, to understand the distribution of heat generated by the electric current. This is different from an actual production situation but understanding these effects is critical to optimizing aluminum production and ensuring stable operation during current variations. Further research will focus on developing control strategies to mitigate the adverse effects of current variations, thereby improving the overall efficiency of cell operation.

#### 5. References

1. Feng Naixiang, *Aluminum Electrolysis* [M], Beijing, Chemical Industry Press, 2006, 78-85.
2. Mei Chi, Wang Qianpu and Wu Lemou, Study on thermal field of aluminum electrolysis cell [J], *Light Metals (Chinese)*, 1992 (1), 29-32.
3. You Wang and Wang Qianpu. Theoretical Study on Online Simulation of Cell Chamber Inner Structure of Aluminum Electrolysis Cell [J]. *The Chinese Journal of Nonferrous Metals*, 1998, 8 (4):695
4. Luo Haiyan, Lu Jidong, et. al. Development of Electrothermal Field Analysis Technology of Aluminum Electrolysis Cell [J], *Light Metals (Chinese)*, 2002 (2), 59.
5. Warren E. Haupin, Interpreting the components of cell voltage, *Light Metals* 1998, 531-537.
6. Abdalla Al Zarouni et al. and Vinko Potocnik, Energy and mass balance in DX+ cells during amperage increase, 494-499.
7. Warren Haupin and Halvor Kvande, Thermodynamics of electrochemical reduction of alumina, *Light Metals* 2000, 379-384.